BMB
reports

Contribution of lysine-containing cationic domains to thermally-induced phase transition of elastin-like proteins and their sensitivity to different stimuli

*Won Bae Jeon**

Laboratory of Biochemistry and Cellular Engineering, Daegu Gyeongbuk Institute of Science and Technology, Daegu 704-230, Korea

A series of elastin-like proteins, SKGPG[V(VKG)$_3$VKVPG]$_n$-(ELP1-90)WP (n = 1, 2, 3, and 4), were biosynthesized based on the hydrophobic and lysine linkage domains of tropoelastin. The formation of self-assembled hydrophobic aggregates was monitored in order to determine the influence of cationic segments on phase transition properties as well as the sensitivity to changes in salt and pH. The thermal transition profiles of the proteins fused with only one or two cationic blocks (n = 1 or 2) were similar to that of the counterpart ELP1-90. In contrast, diblock proteins that contain 3 and 4 cationic blocks displayed a triphasic profile and no transition, respectively. Upon increasing the salt concentration and pH, a stimulus-induced phase transition from a soluble conformation to an insoluble aggregate was observed. The effects of cationic segments on the stimuli sensitivity of cationic bimodal ELPs were interpreted in terms of their structural and molecular characteristics. [BMB reports 2011; 44(1): 22-27]

INTRODUCTION

Elastin is a major component of elastic fibers found in the extracellular matrix of many tissues, for which elasticity is of great importance (1). Elastin is an insoluble molecule formed from many monomers of water-soluble tropoelastin. Tropoelastin is encoded by a single-copy gene, but alternative splicing of transcripts results in various isomeric forms of the protein, each with a molecular weight of approximately 70 kDa (2). The primary structure of tropoelastin consists of alternating hydrophobic and cross-linking domains. The hydrophobic domains are composed of repeats of alternating hydrophobic amino acid sequences such as VPGVG and APGVGV, whereas the AK cross-linking domains consist mainly of Ala and Lys, e.g., AAAAKAAKYGA (3). Under physiological conditions, the hydrophobic domains of tropoelastin undergo a self-assembly process that is referred to as coacervation (4), and the resulting assembly is stabilized by the formation of intermolecular cross-links between Lys residues that produce a highly insoluble network of elastic fibers (5).

Protein-based polymers that respond to biologically relevant stimuli by altering their conformation or properties are often considered to be intelligent or smart biomaterials (6). In particular, elastin-like proteins (ELPs) that are modeled on the VPGXG pentapeptide repeat of tropoelastin, in which X is any amino acid except proline, display a soluble-insoluble phase transition in response to changes in temperature, salt, or pH, and thus have emerged as promising smart proteins for biomedical applications (7, 8). The temperature at which the soluble-insoluble conformational change occurs, known as the inverse transition temperature (T_t), has been used to characterize the responsiveness of ELPs to a change in stimulating factors (9). ELPs are highly compatible with living cells; therefore, they have high potential for use in the delivery of drugs or genes or as a matrix for mammalian cell culture or wound healing (10, 11). However, owing to the low chemical reactivity of hydrophobic VPGXG units, the biological utilization of unmodified forms of ELPs is limited. As a consequence, functionalized ELPs have been generated by conjugating or incorporating biologically active sequences into the structural backbone of ELPs (12). For example, fusion of homing peptides or affinity ligands to the N- or C-terminus of ELPs (13), which produces a multimodal form (14), enables receptor-mediated targeting of these proteins to biologically relevant sites. Similarly, the ability of the proteins to bind and deliver drugs can be further modulated by fusing the ELP backbone to an anionic or cationic domain. Such cationic or anionic ELPs not only provide amino or carboxylic groups for the covalent conjugation of drug cargos but also are able to self-assemble into a hydrogel or micelle structure. Furthermore, the size of micellar particles can be modulated by selecting cationic or anionic domains of different sequence and number, which is of great interest in targeting cancer drugs by local hyperthermia (15) or the development of intelligent gene delivery

*Corresponding author. Tel: 82-53-430-8582; Fax: 82-53-431-8605;
E-mail: wbjeon@dgist.ac.kr
DOI 10.5483/BMBRep.2011.44.1.22

Received 2 August 2010, Accepted 30 September 2010

Keywords: Cationic diblock biopolymers, Elastin-like proteins, Intelligent biomaterials, Inverse phase transition, Micellar assembly

vehicles (16, 17). Therefore, detailed characterization of the phase transition properties of cationic ELPs under various environmental conditions is necessary as it will provide insights into the precise control of physicochemical properties. Previously, an elastin-based polylysine diblock biopolymer, K_8ELP1-60, was tested as a vehicle for thermally targeted chemotherapy or gene delivery (15-17). However, there are no reports in the literature of the effect of cationic domains on the sensitivity of bimodal ELPs to stimuli.

The aim of the study described herein was to investigate the effects of lysine-containing cationic domains by characterizing the phase transition properties of a set of diblock cationic ELPs, SKGPG[V(VKG)$_3$VKVPG]$_n$-ELP1-90, which mimic both the cross-linking and hydrophobic domains of tropoelastin. Determining the characteristics of these cationic ELPs with respect to responsiveness towards changes in temperature, ionic strength, and pH should reveal useful information on the mechanisms responsible for the behavior of amphiphilic ELPs under various solution conditions, and ultimately aid in the design of protein-based intelligent biomaterials that respond to changes in environmental stimuli.

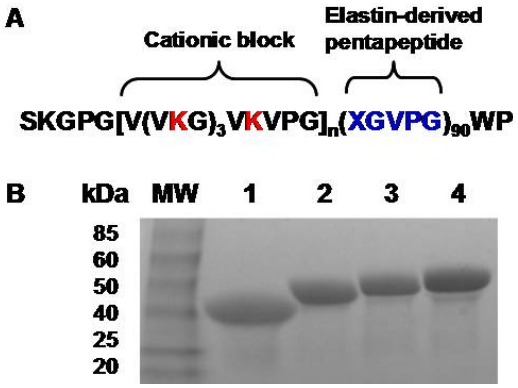

Fig. 1. Schematic illustration of bimodal composition of cationic ELPs (A), and SDS-PAGE analysis of the purity and MW of the isolated proteins (B). Lanes 1, 2, 3, and 4 represent [V(VKG)$_3$VKVPG]$_n$-ELP1-90 with n = 1, 2, 3, and 4, respectively.

RESULTS

Design and production of cationic diblock elastin-like proteins

In order to analyze the effects of cationic domains on the sensitivity of cationic ELPs in response to a change in environmental stimuli, a set of diblock ELPs, SKGPG[V(VKG)$_3$VKVPG]$_n$[(VGVPG)$_2$GGVPGAGVPG(VGVPG)$_3$GGVPGAGVPGGGVPG]$_9$WP (n = 1, 2, 3, and 4), was biosynthesized (hereafter referred to as [V(VKG)$_3$VKVPG]$_n$-ELP1-90). In each diblock ELP, a cationic unit contained four lysine residues, and the ELP1-90 segment consisted of 90 repeats of the XGVPG pentapeptide, in which X corresponds to Val, Ala, and Gly in a 5 : 2 : 3 molar ratio. The unit V(VKG)$_3$VKVPG was designed such that it generated rigid VPGVV and VPGVG sequences upon formation of cationic domains and was connected to the ELP1-90 segment.

DNA sequences that encode [V(VKG)$_3$VKVPG]$_n$-ELP1-90 were cloned successfully by recursive directional ligation (RDL, 18), and the bimodal ELPs were expressed and purified from *E. coli*. Three rounds of inverse transition cycling yielded [V(VKG)$_3$VKVPG]$_n$ELP1-90 of purity greater than 95%, as judged by SDS-PAGE (Fig. 1B). When compared to the MW of the standard proteins, the purified proteins migrated to positions that corresponded to a slightly larger MW than that of the calculated value, a trend that was reported previously (19). However, when the expressed proteins were compared to each other, the differences in relative migration distance were consistent with the expected differences in MW. During SDS-poly-

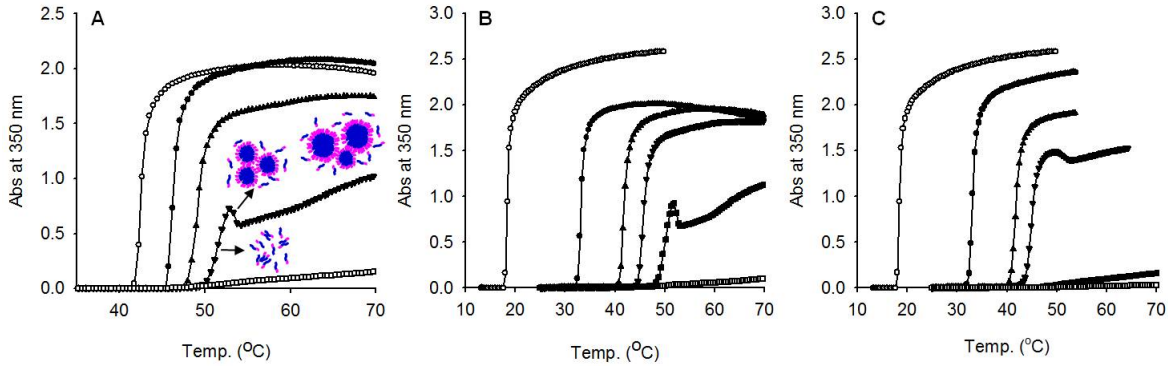

Fig. 2. Turbidity profiles obtained for ELP1-90 (○) and [V(VKG)$_3$VKVPG]$_n$-ELP1-90 [n = 1 (●), 2 (▲), 3 (▼), and 4 (□)] (A). Inverse temperature transition of [V(VKG)$_3$VKVPG]$_3$-ELP1-90 (B) and [V(VKG)$_3$VKVPG]$_4$-ELP1-90 (C) in the presence of 50 (□), 100 (■), 300 (▼), 500 (▲), 1,000 (●), and 2,000 (○) mM NaCl. The concentration of cationic ELPs was 25 μM in 10 mM phosphate buffer. In the cartoon of graph A, pink and blue represent [V(VKG)$_3$VKVPG]$_3$ block in solution and ELP1-90 domain out of solution, respectively.

Table 1. Summaries of protein properties and effects of salt and pH on T_t values

Protein	MW (Da)	pI	CCD* (%)	T_t†	Conc. of NaCl (mM)						pH						
					0.05	0.1	0.3	0.5	1	2	6	7	8	9	10	11	12
ELP1-90	35,940	8.5	0	42.2	ND‡						ND						
V(VKG)$_3$VKVPG-ELP1-90	37,373	10.6	4.0	44.9	49.1	48.4	42.5	38.8	32.2	21.0	44.1	44.5	45.4	46.6	50.5	48.6	47.6
[V(VKG)$_3$VKVPG]$_2$-ELP1-90	38,806	10.9	7.8	47.2	TT§	46.9	43.2	39.7	31.9	19.9	47.3	47.0	48.2	48.9	52.1	47.8	47.7
[V(VKG)$_3$VKVPG]$_3$-ELP1-90	40,238	11.1	11.2	50.4	NT‖	TT	45.4	41.6	32.9	18.0	50.0	49.6	50.1	50.2	50.2	53.7	46.9
[V(VKG)$_3$VKVPG]$_4$-ELP1-90	41,671	11.2	13.9	NT	NT	NT	44.8	41.7	327	18.0	NT	NT	ND	ND	ND	ND	47.7

*Content of cationic domains in a molecule (MW of cationic domains/MW of molecule ×100), †T_t at 25 μM of protein in PBS, ‡Not determined, §Triphasic transition, ‖No transition

acrylamide gel electrophoresis, the migration rate of a protein is affected not only by its size but also by shape. In SDS-PAGE buffer, an ELP may have an extended conformation, which could result in a slower migration rate than that of a globular protein standard having the same MW. Approximately 25 mg of purified cationic ELP was obtained from 1 L of culture, and the yield did not differ among the four ELPs, which indicates that the cationic domains did not have an adverse effect on the production of the diblock ELPs.

Transition characteristics of bimodal ELPs

The phase transition properties of the diblock ELPs (25 μM) in PBS are depicted in Fig. 2A. ELP1-90 showed a very sharp increase in turbidity with a T_t of 42°C. V(VKG)$_3$VKVPG-ELP1-90 and [V(VKG)$_3$VKVPG]$_2$-ELP1-90 also displayed a rapid increase in turbidity, although their T_t values were shifted to higher temperatures of 45°C and 47°C, respectively. In contrast, the turbidity profile of [V(VKG)$_3$VKVPG]$_3$-ELP1-90 exhibited a triphasic transition: the first slow transition with a T_t of 50°C was followed by a rapid drop in absorbance between 53°C and 56°C, and then a gradual increase in turbidity above 56°C. In the case of [V(VKG)$_3$VKVPG]$_4$-ELP1-90, an inverse temperature transition was not observed. Table 1 summarizes the relationship between the number of cationic domains and the T_t values of the cationic ELPs. As the number of cationic domains in the ELP molecule increased, the T_t of the ELP shifted to a higher temperature with a concomitant decrease in the degree of thermal sensitivity.

Sensitivity to salt concentration

The influence of salt concentration on the phase transition properties of the cationic ELPs was investigated using [V(VKG)$_3$VKVPG]$_3$ELP1-90 and [V(VKG)$_3$VKVPG]$_4$-ELP1-90 in 10 mM phosphate buffer (pH 7.4) (Fig. 2B, C), since neither ELP was sensitive to temperature change at 50 mM NaCl. In 100 mM NaCl, [V(VKG)$_3$VKVPG]$_3$-ELP1-90 showed a triphasic transition profile, whereas [V(VKG)$_3$VKVPG]$_4$ELP1-90 remained insensitive to thermal change. In the presence of 300 mM NaCl, [V(VKG)$_3$VKVPG]$_4$ELP1-90 became responsive to temperature change. As the concentration of NaCl was increased higher than 500 mM, both [V(VKG)$_3$VKVPG]$_3$ELP1-90 and [V(VKG)$_3$VKVPG]$_4$ELP1-90 became fully thermosensitive and showed similar T_t values of around 42°C. Any further increase in NaCl concentration up to 2 M resulted in a shift of T_t to 18°C along with enhancement in the slope of the transition curves.

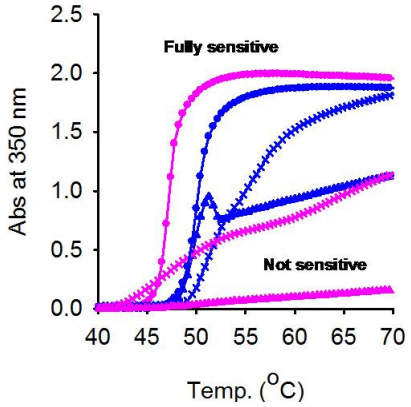

Fig. 3. Solution turbidity of [V(VKG)$_3$VKVPG]$_3$-ELP1-90 (blue) and [V(VKG)$_3$VKVPG]$_4$-ELP1-90 (pink) at pH 7.0 (▲), 10.0 (x), and 12.0 (●). The concentration of cationic ELPs was 25 μM in PBS, and the heating rate was 1°C/min.

pH responsiveness

Fig. 3 illustrates the sensitivity of [V(VKG)$_3$VKVPG]$_n$ELP1-90 (n = 3 or 4) to pH change. At pH 7.0, [V(VKG)$_3$VKVPG]$_3$ELP1-90 showed a triphasic transition profile. As the pH was increased to 10, the phase transition profile became hyperbolic, which indicates that thermal responsiveness was enhanced. At pH 12, the transition curve exhibited a sigmoidal shape with a T_t of 47°C. Similar results were obtained for [V(VKG)$_3$VKVPG]$_4$-ELP1-90. The latter did not display phase transition at pH 7.0, although it was fully responsive to temperature change at pH 12.0 with a T_t of 48°C. The finding that the T_t value at pH 12.0 was lower for [V(VKG)$_3$VKVPG]$_4$-ELP1-90 than for [V(VKG)$_3$VKVPG]$_3$ELP1-90 suggests that there were more intermolecular interactions in the case of [V(VKG)$_3$VKVPG]$_4$-ELP1-90 since the

uncharged ELP chain length had increased. This result is consistent with a report that found T_t decreases as the chain length of a hydrophobic ELP molecule increases (20). Table 1 summarizes the influence of the number of cationic domains on the phase transition properties of diblock ELPs as well as on their sensitivity to stimuli.

DISCUSSION

The self-assembly or coacervation of ELPs in solution occurs via a mechanism that involves a conformational change from a random chain into a β-turn conformation, hydrophobic association, and a maturation process into larger aggregates (21). Within diblock ELPs, which are composed of two different ELP segments with different T_t values, the ELP block with the lower T_t value assumes the β-turn conformation and collapses above its T_t, whereas the other segment with the higher T_t value remains in solution (18). On the basis of these investigations, it is plausible that the observed triphasic thermal transition for $[V(VKG)_3VKVPG]_3$-ELP1-90 indicates the formation of a core-shell micelle structure. When the temperature is increased close to the T_t of 50°C, the solvated hydrophobic ELP1-90 segment undergoes a conformational change to form a β-turn structure. Upon a further increase in temperature above the T_t, intermolecular hydrophobic interactions between the β-turn coils of the ELP1-90 segments cause the proteins to assemble into a micelle structure, in which the ELP1-90 segments form a hydrophobic core surrounded by a hydrophilic shell of solvated cationic sequences. It is likely that the sudden linear drop in turbidity of the solution between 53°C and 56°C is caused by the rearrangement of small particles into micelle structures, whereas the gradual increase in turbidity observed between 56°C and 70°C may be due to the formation of supramolecular aggregates at the expense of small micelles (Cartoon of Fig. 2A). Dynamic particle size monitoring during the phase transition process of $[V(VKG)_3VKVPG]_3$-ELP1-90 could provide evidence to support this interpretation.

In analyzing the contribution of lysine-containing domains to the salt sensitivity of cationic ELPs, the addition of NaCl caused a concentration-dependent decrease in T_t along with an increase in the thermal sensitivity of cationic ELPs at neutral pH, at which they have a net positive charge. High NaCl concentrations (>500 mM) were necessary to induce phase transition of cationic ELPs whose hydrophilic cationic content was higher than 10%, indicating that NaCl enhanced the hydrophobic interaction of ELP molecules. It has been suggested that Cl^- ions destabilize water molecules that are involved in hydrophobic hydration and order themselves surrounding the hydrophobic pentapeptide of ELPs under thermally-induced phase transition (22). However, in the case of $[V(VKG)_3VKVPG]_3$-ELP1-90 and $[V(VKG)_3VKVPG]_4$-ELP1-90, the observed increase in thermal sensitivity at high concentrations of NaCl may partly be the result of a shielding or neutralizing effect of Cl^- counter ions on the positively charged ε-amino groups of lysine residues. This would reduce electrostatic repulsion at the interfaces of the cationic domains as well as decrease the interaction between the cationic domain and water molecules, thus improving the formation of ordered water structures around the cationic domains. For the cationic ELPs, the apparent increase in temperature sensitivity would be a combined effect of the two mechanisms.

From the perspective of molecular structure, the pH versus transition profiles show that the pH responsiveness of $[V(VKG)_3VKVPG]_n$-ELP1-90 (where n = 1 and 2) was due to the overall balance between the charged and uncharged ionic states exhibited by the ε-amino group of lysine. At pH 7.0, the thermal sensitivity of $[V(VKG)_3VKVPG]_3$ELP1-90 was lower than that of its counterpart ELP1-90, whereas $[V(VKG)_3VKVPG]_4$-ELP1-90 demonstrated no transition. This may have been caused by electrostatic repulsion at the cationic interfaces or by positively charged cationic domains preventing the packing of hydrophobic β-turns between ELP segments. As the pH was increased to 10.0, both $[V(VKG)_3VKVPG]_3$-ELP1-90 and $[V(VKG)_3VKVPG]_4$-ELP1-90 demonstrated an enhanced responsiveness to thermal change, whereas at pH 12.0, the cationic ELPs exhibited a rapid response. This behavior correlates with the degree of ionization of the lysine side chains, which have a pI of 10.3. The pI values of $[V(VKG)_3VKVPG]_3$-ELP1-90 and $[V(VKG)_3VKVPG]_4$-ELP1-90 were 11.1 and 11.2, respectively (Table 1). Therefore, at pH <12.0, the side chains were fully deprotonated and uncharged. Hence, the entire molecular structure had no net charge, in contrast to the protonated state at pH 7.0; the uncharged structure facilitated hydrophobic interactions between ELP segments at a lower temperature.

In conclusion, the results of this study show that the sensitivity of ELPs to stimuli can be modulated by changing the sequence and number of cationic blocks fused to a thermally responsive ELP segment. Such control over sensitivity to stimuli by the fusion of charged domains could broaden the field of ELP applications, in which sensitivities to temperature, salt, and pH are highly desirable.

MATERIALS AND METHODS

Construction of the coding sequence for the $V(VKG)_3VKVPG$ unit

Two oligonucleotides (forward: 5'-AATTCCCACGGCGTGGTTAAAGGTGTTAAAGGTGTTAAAGGTGTTAAAGTGCCGGGCGGGCA-3' and reverse: 5'-AGCTTGCCCGCCCGGCACTTTAACACCTTTAACACCTTTAACACCTTTAACCACGCCGTGGG-3') encoding the $V(VKG)_3VKVPG$ monomeric block unit were designed such that *Eco*RI, *Pfl*MI, *Bgl*I, and *Hin*DIII restriction enzyme sites were generated upon annealing to form a double-stranded DNA fragment. A double-stranded DNA cassette was formed by heating a mixture of the two oligonucleotides in ligase buffer at 95°C for 5 min, followed by cooling to room temperature at a rate of 1°C/min. The cloning vector pUC19 (NEB) was digested with both *Eco*RI and *Hin*DIII (NEB) and de-

phosphorylated using calf intestinal phosphatase (CIP; Promega). The linearized pUC19 vector was then purified from an agarose gel using a spin column purification kit (Qiagen) and ligated with the double-stranded DNA cassette for $V(VKG)_3$ VKVPG. After ligation, *E. coli* Top 10 cells (Invitrogen) were transformed with the ligation product by the heat shock method, spread on CircleGrow agar medium (Q-BIO gene) supplemented with ampicillin (100 μg/ml), and incubated overnight at 37°C. Multiple colonies were chosen and grown in 5 ml of CircleGrow medium with ampicillin for 12 hrs at 37°C. Plasmids were isolated and purified from the 5 ml cultures using a miniprep kit (Qiagen). A clone containing the recombinant plasmid with the correct insert was identified by diagnostic digestion using *Eco*RI, *Pfl*MI, and *Hin*DIII.

Construction of the coding sequence for the $[V(VKG)_3VKVPG]_n$ domain

DNA fragments encoding $[V(VKG)_3VKVPG]_n$, where n = 1, 2, 3, or 4, were prepared from the plasmid containing $V(VKG)_3$ VKVPG gene by applying RDL (18). Briefly, pUC19, containing the sequence for the $V(VKG)_3VKVPG$ monomeric unit, was linearized with *Pfl*MI, dephosphorylated with CIP, and the fragments separated on an agarose gel. The linearized plasmid was purified from the gel using a spin column purification kit (Qiagen). A separate sample of the plasmid was digested with both *Pfl*MI and *Bgl*I in order to liberate the sequence encoding the $V(VKG)_3VKVPG$ monomer. After digestion, the reaction products were separated by high-melting agarose gel electrophoresis, after which the insert was purified using a DNA extraction kit (Qiagen). The purified insert was then ligated into the linearized pUC19 vector, and the resulting product was transformed into *E. coli* Top10 cells. Transformants were screened initially by diagnostic digestion using *Eco*RI and *Hin*DIII and further confirmed by DNA sequencing. A clone containing the sequence for the $[V(VKG)_3VKVPG]_2$ peptide was identified and selected for the next round of RDL. Additional rounds were performed in an identical manner using the construct from the previous round as the starting clone.

Construction of the $[V(VKG)_3VKVPG]_n$-ELP1-90 gene library

A pUC19-based cloning vector, pUC19-ELP1-90, containing a copy of the coding sequence for ELP1-90, was prepared in accordance with a previously published method (18). The vector was digested with *Pfl*MI, dephosphorylated with CIP, and separated on an agarose gel, after which the linearized plasmid was purified from the gel using a spin DNA extraction kit. A separate pUC19 vector containing the gene for $[V(VKG)_3$ $VKVPG]_n$ was digested with both *Pfl*MI and *Bgl*I in order to liberate the target insert. After digestion, the reaction products were separated on by agarose gel electrophoresis, and the insert was purified from the gel using a DNA extraction kit. The pET-25b(+)SV2 vector (18) was linearized by digestion with *Sfi*I, dephosphorylated with CIP, and then purified by agarose gel extraction after electrophoresis. The purified $[V(VKG)_3VKVPG]_n$ gene along with the linearized pET-25b(+)SV2 vector were ligated (20 pmol of vector and 100 pmol of insert incubated in 20 μl of ligase buffer with 10 units of ligase from NEB) at 16°C for 5 hrs, after which the ligation mixture was transformed into *E. coli* Top10 cells. Plasmids isolated from the resulting transformants were screened by diagnostic digestion with *Ava*I and *Xba*I (NEB), and the identity of the insert was then confirmed further by DNA sequencing. The plasmids containing the coding sequences for the diblock $[V(VKG)_3VKVPG]_n$-ELP1-90 polymer were transformed into *E. coli* strain BLR(DE3) by the heat shock method.

Expression and purification of cationic ELPs

E. coli BLR(DE3) transformed with the pET-based expression vector containing the coding sequence for $[V(VKG)_3VKVPG]_n$ ELP1-90 was grown in CircleGrow medium at 37°C for 24 hrs. After harvesting, cells were disrupted by sonication, and the diblock ELPs were purified from the cell lysate by the inverse transition cycling (ITC) method as described previously (19). Protein concentrations were determined by UV spectrophotometry using a molar extinction coefficient of 5,690 M^{-1} cm^{-1} for a single Trp residue at 280 nm (18). The purified proteins were dissolved in PBS (pH 7.4; Gibco) at a concentration of 20 mg/ml and kept at −80°C until use. The purity and molecular weight of the cationic ELPs were analyzed by visualization on a 12% SDS-PAGE gel using Coomassie Brilliant Blue R-250 stain (Bio-Rad). The molecular weights (MWs) of the $[V(VKG)_3$ $VKVPG]_n$ELP1-90 polymers were computed using Compute pI/MW software, which is available from the ExPASy Proteomics Server.

Characterization of sensitivity to stimuli by inverse temperature transition

The effects of cationic domain content, salt, and pH on the thermally induced phase transition of $[V(VKG)_3VKVPG]_n$ELP1-90 were characterized by monitoring the optical density of protein solutions at 350 nm as a function of temperature on a Cary 100 UV-visible spectrophotometer equipped with a multicell thermoelectric temperature controller (Varian). The rate for heating and cooling of the temperatures was 1°C/min, and the T_t was determined as the temperature at which half maximum optical density was observed.

Acknowledgments

This work was supported partly by the Biodefense Program Fund to WBJ from the Ministry of Education, Science and Technology of the Republic of Korea.

REFERENCES

1. Rogenbloom, J., Abrams, W. R. and Mecham R. (1993) Exracellular matrix 4: the elastic fiber. *FASEB J.* **7**, 1208-1218.
2. Bashir, M. M., Indik, Z., Yeh, H., Ornstein-Goldstein, N.,

Rosenbloom, J. C., Abrams, W., Fazio, M., Uitto, J. and Rosenbloom, J. (1989) Characterization of the complete human elastin gene. Delineation of unusual features in the 5-flanking region. *J. Biol. Chem.* **264**, 8887-8891.
3. Brown-Augsburgert, P., Tisdale, C., Broekelmann, T., Sloan, C. and Mecham, R. P. (1995) Identification of an elastin cross-linking domain that joins three peptide chains. *J. Biol. Chem.* **270**, 17778-17783.
4. Clarke, A. W., Arnspang, E. C., Mithieux, S. M., Korkmaz, E., Braet, F. and Weiss, S. A. (2006) Tropoelastin massively associates during coacervation to form quantized protein spheres. *Biochemistry* **45**, 9989-9996.
5. Kielty, C. M., Sherratt, M. J. and Shuttleworth, C. A. (2002) Elastic fibres. *J. Cell Sci.* **115**, 2817-2828.
6. Mart, R. J., Osborne, R. D., Stevens, M. M. and Ulijn, R. V. (2006) Peptide-based stimuli-responsive biomaterials. *Soft Matter* **2**, 822-835.
7. Chilkoti, A., Christensen, T. and MacKay, J. A. (2006) Stimulus responsive elastin biopolymers: applications in medicine and biotechnology. *Curr. Opin. Chem. Biol.* **10**, 652-657.
8. Furth, M. E., Atala, A. and Van Dyke, M. E. (2007) Smart biomaterials design for tissue engineering and regenerative medicine. *Biomaterials* **28**, 5068-5073.
9. Urry, D. A. (1997) Physical chemistry of biological free energy transduction as demonstrated by elastic protein-based polymers. *J. Phys. Chem. B* **101**, 11007-11028.
10. Herrero-Vanrell, R., Rincón, A. C., Alonso, M., Reboto, V., Molina-Martinez, I. T. and Rodríguez-Cabello, J. C. (2005) Self-assembled particles of an elastin-like polymer as vehicles for controlled drug release. *J. Control. Release* **102**, 113-122.
11. McHale, M. K., Setton, L. A. and Chilkoti, A. (2005) Synthesis and *in vitro* evaluation of enzymatically cross-linked elastin-like polypeptide gels for cartilaginous tissue repair. *Tissue Eng.* **11**, 1768-1779.
12. Nicol, A., Gowda, D. C. and Urry, D. W. (1992) Cell adhesion and growth on synthetic elastomeric matrices containing Arg-Gly-Asp-Ser-3. *J. Biomed. Mater. Res. A* **26**, 393-413.
13. Massodi, I., Bidwell III, G. L. and Raucher, D. (2005) Evaluation of cell penetrating peptides fused to elastin-like polypeptide for drug delivery. *J. Control. Release* **108**, 396-408.
14. Straley, K. and Heilshorn, S. C. (2009) Design and adsorption of modular engineered proteins to prepare customized, neuron-compatible coatings. *Front Neuroengineering* **2**, 1-10.
15. Bae, Y., Buresh, R. A., Williamson, T. P., Chen, T. H. and Furgeson, D. Y. (2007) Intelligent biosynthetic nanobiomaterials for hyperthermic combination chemotherapy and thermal drug targeting of HSP90 inhibitor geldanamycin. *J. Control. Release* **122**, 16-23.
16. Chen, T. H., Bae, Y. and Furgeson, D. Y. (2008) Intelligent biosynthetic nanobiomaterials (IBNs) for hyperthermic gene delivery. *Pharm. Res.* **25**, 683-691.
17. Haider, M., Leung, V., Ferrari, F., Crissman, J., Powell, J., Cappello, J. and Ghandehari, H. (2005) Molecular engineering of silk-elastin-like polymers for matrix-mediated gene delivery: biosynthesis and characterization. *Mol. Pharm.* **2**, 139-150.
18. Meyer, D. E. and Chilkoti, A. (2002) Genetically encoded synthesis of protein-based polymers with precisely specified molecular weight and sequence by recursive directional ligation: examples from the elastin-like polypeptide system. *Biomacromolecules* **3**, 357-367.
19. McPherson, D. T., Xu, J. and Urry, D. W. (1996) Product purification by reversible phase transition following Escherichia coli expression of genes encoding up to 251 repeats of the elastomeric pentapeptide GVGVP. *Protein Expr. Purif.* **7**, 51-57.
20. Meyer, D. E. and Chilkoti, A. (2004) Quantification of the effects of chain length and concentration on the thermal behavior of elastin-like polypeptides. *Biomacromolecules* **5**, 846-851.
21. Yamaoka, T., Tamura, T., Seto, Y., Tada, T., Kunugi, S. and Tirrell, D. A. (2003) Mechanism for the phase transition of a genetically engineered elastin model peptide $(VPGIG)_{40}$ in aqueous solution. *Biomacromolecules* **4**, 1680-1685.
22. Cho, Y., Zhang, Y., Christensen, T., Sagle, L. B., Chilkoti, A. and Cremer P. S. (2008) Effects of Hofmeister anions on the phase transition temperature of elastin-like polypeptides. *J. Phys. Chem. B* **112**, 13765-13771.